

# A Comparison of Latent Semantic Analysis and Correspondence Analysis for Text Mining

Qianqian Qi  
Utrecht University  
q.qi@uu.nl

David J. Hessen  
Utrecht University  
d.j.hessen@uu.nl

Peter G. M. van der Heijden  
Utrecht University and University of Southampton  
P.G.M.vanderHeijden@uu.nl

**Abstract:** Both latent semantic analysis (LSA) and correspondence analysis (CA) use a singular value decomposition (SVD) for dimensionality reduction. In this article, LSA and CA are compared from a theoretical point of view and applied in both a toy example and an authorship attribution example. In text mining interest goes out to the relationships among documents and terms: for example, what terms are more often used in what documents. However, the LSA solution displays a mix of marginal effects and these relationships. It appears that CA has more attractive properties than LSA. One such property is that, in CA, the effect of the margins is effectively eliminated, so that the CA solution is optimally suited to focus on the relationships among documents and terms. Three mechanisms are distinguished to weight documents and terms, and a unifying framework is proposed that includes these three mechanisms and includes both CA and LSA as special cases. In the authorship attribution example, the national anthem of the Netherlands, the application of the discussed methods is illustrated.

**Keywords:** Latent semantic analysis; Correspondence analysis; Singular value decomposition; Authorship attribution; *Wilhelmus*.

## 1 Introduction

Latent semantic analysis (LSA) is a popular method for dimensionality reduction in text mining (Aggarwal, 2018). It is originally designed for improving information retrieval by using the associations between documents and terms (Deerwester, Dumais, Furnas, Landauer, & Harshman, 1990; Dumais, 1991; Dumais, Furnas, Landauer, Deerwester, & Harshman, 1988). Correspondence analysis (CA) is a popular method for the analysis of contingency tables (Greenacre, 1984, 2017). It provides a graphic display of dependence between the rows and columns of a two-way contingency table (Greenacre & Hastie, 1987). Like LSA, CA is a dimensionality reduction method. The methods have much in common as both use singular value decomposition (SVD). After dimensionality reduction, text mining tasks, such as text clustering, may be performed in the reduced dimensional space rather than in the higher dimensional space provided by the raw document-term matrix.

Several comparisons of LSA and CA can be found in the literature. For example, Morin (1999) compared the two methods in the automatic exploration of themes in texts. Séguéla and Saporta (2011) compared the performance of CA and LSA with several weighting functions in a clustering task, and found a good performance of CA. Séguéla and Saporta (2013) also compared the performance of both CA and LSA with TF-IDF on a recommender system, and found that the quality provided by CA is slightly less. Another comparison can be found in Murtagh, Pianosi, and Bull (2016). However, overseeing the literature a comprehensive theoretical comparison between LSA and CA is lacking.

In the present article, therefore, a theoretical comparison of LSA and CA is provided and the two techniques are placed in a unifying framework. It is shown that CA has some favorable properties not shared by LSA. The use of LSA and CA is explored by studying the unknown authorship of the *Wilhelmus*, the national anthem of the Netherlands written in the 16th century. The text of the *Wilhelmus* is compared with texts from a set of writers that lived at the time the *Wilhelmus* was written (Kestemont, Stronks, De Bruin, & Winkel, 2017a, 2017b; Winkel, 2015).

The rest of the article is organized as follows. In Section 2, we simply present properties of a document-term matrix by using a small dataset. Section 3 and Section 4 elaborate LSA and CA and apply them on the small dataset. A unifying framework is proposed in Section 5. Authorship attribution of the *Wilhelmus* is explored in Section 6. The article ends with a discussion.

## 2 Data

In many applications of text mining, document-term matrices are analyzed. Document-term matrices have specific properties that are relevant for a theoretical comparison of LSA and CA. In this section, these properties are discussed.

Suppose  $\mathbf{F} = [f_{ij}]$  is a document-term matrix of size  $m \times n$ , in which rows correspond to documents, columns are associated with terms, and an element is the frequency of occurrence of a term in a particular document. The matrix  $\mathbf{P} = [p_{ij}]$  is the matrix of joint observed proportions, where the element in the  $i$ th row and the  $j$ th column is given by  $p_{ij} = f_{ij} / \sum_i \sum_j f_{ij}$  and  $\sum_i \sum_j p_{ij} = 1$ . The marginal proportions are denoted by  $r_i$  and  $c_j$  for the  $i$ th row and  $j$ th column respectively, where  $r_i = \sum_{j=1}^n p_{ij}$ ,  $c_j = \sum_{i=1}^m p_{ij}$ . For row  $i$ , the vector of  $n$  conditional proportions  $p_{ij}/r_i$  is called a row profile. Similarly, for column  $j$  the vector of  $m$  conditional proportions  $p_{ij}/c_j$  is called the column profile. The vector with elements  $c_j$  is called the average row profile, and similarly, the vector with elements  $r_i$ , the average column profile.

The relationships between documents and terms can be studied in three ways: (1) by comparing the joint proportions with the product of marginal proportions, for example, if  $p_{ij} > r_i c_j$ , then term  $j$  appears in document  $i$  more often than expected from the margins and if  $p_{ij} < r_i c_j$ , then it appears less often than expected; (2) by comparing the elements of  $i$ th row profile with the average row profile, for example, when  $p_{ij}/r_i > c_j$ , then term  $j$  appears in document  $i$  more often than average; and (3) by comparing the elements of  $j$ th column profile with the average column profile, for example, when  $p_{ij}/c_j > r_i$ , then term  $j$  appears more often than average in document  $i$ .

Consider the  $6 \times 6$  document-term matrix  $\mathbf{F}$  in Table 1 (Aggarwal, 2018). It contains 6 documents and for each document, we are interested in the frequency of occurrence of six terms. The first three documents primarily refer to cats, the last two primarily to cars, and the fourth to both. The fourth term, jaguar, is polysemous because it can refer to either a cat or a car. Table 2 shows the matrix  $\mathbf{P}$  of joint observed proportions. Here,

Table 1: A document-term matrix  $F$ : size  $6 \times 6$

	lion	tiger	cheetah	jaguar	porsche	ferrari
doc1	2	2	1	2	0	0
doc2	2	3	3	3	0	0
doc3	1	1	1	1	0	0
doc4	2	2	2	3	1	1
doc5	0	0	0	1	1	1
doc6	0	0	0	2	1	2

the average column profile is  $r = [0.171, \dots, 0.122]^T$  and the average row profile is  $c = [0.171, \dots, 0.098]^T$ .

Table 2: The matrix  $P$  of joint observed proportions

	lion	tiger	cheetah	jaguar	porsche	ferrari	total
doc1	0.049	0.049	0.024	0.049	0.000	0.000	0.171
doc2	0.049	0.073	0.073	0.073	0.000	0.000	0.268
doc3	0.024	0.024	0.024	0.024	0.000	0.000	0.098
doc4	0.049	0.049	0.049	0.073	0.024	0.024	0.268
doc5	0.000	0.000	0.000	0.024	0.024	0.024	0.073
doc6	0.000	0.000	0.000	0.049	0.024	0.049	0.122
total	0.171	0.195	0.171	0.293	0.073	0.098	1.000

Table 3 shows the matrix  $E$  of expected proportions under independence. Under independence,  $e_{ij} = r_i c_j$ , and all row profiles are identical as  $e_{ij}/r_i = r_i c_j/r_i = c_j$ , and similarly for the column profiles. Comparing the joint proportions in Table 2 with these expected proportions in Table 3 reveals how documents are related to terms. For instance, the joint proportions for document 1 and lion and document 1 and tiger are (0.049, 0.049) and are higher than their expected proportions (0.029, 0.033), which means that the terms lion and tiger appear more often than average in document 1. However, for document 1 and porsche and document 1 and ferrari, the joint proportions are 0.000 and 0.000 and are lower than their expected joint proportions (0.012, 0.017), which indicates that the terms porsche and ferrari appear less often than average in document 1.

Table 3: The matrix  $E$  of expected proportions under independence

	lion	tiger	cheetah	jaguar	porsche	ferrari	total
doc1	0.029	0.033	0.029	0.050	0.012	0.017	0.171
doc2	0.046	0.052	0.046	0.079	0.020	0.026	0.268
doc3	0.017	0.019	0.017	0.029	0.007	0.010	0.098
doc4	0.046	0.052	0.046	0.079	0.020	0.026	0.268
doc5	0.012	0.014	0.012	0.021	0.005	0.007	0.073
doc6	0.021	0.024	0.021	0.036	0.009	0.012	0.122
total	0.171	0.195	0.171	0.293	0.073	0.098	1.000

Table 4 shows the row profiles. The average row profile shows which terms are more and which are less often used: jaguar is used most and porsche is used least over all the

Table 4: Row profiles of  $F$ 

	lion	tiger	cheetah	jaguar	porsche	ferrari	total
doc1	0.286	0.286	0.143	0.286	0.000	0.000	1.000
doc2	0.182	0.273	0.273	0.273	0.000	0.000	1.000
doc3	0.250	0.250	0.250	0.250	0.000	0.000	1.000
doc4	0.182	0.182	0.182	0.273	0.091	0.091	1.000
doc5	0.000	0.000	0.000	0.333	0.333	0.333	1.000
doc6	0.000	0.000	0.000	0.400	0.200	0.400	1.000
average row profile	0.171	0.195	0.171	0.293	0.073	0.098	1.000

documents. Differences in row profiles between documents can be interpreted by comparing the elements of the row profiles with the average row profile. For example, document 1 has proportions (0.286, 0.286) for lion, tiger and these are higher than the averages (0.171, 0.195); on the other hand, document 5 has proportions (0.000, 0.000) for lion, tiger and these are lower than the averages (0.171, 0.195). This shows that the terms lion and tiger appear more often than average in document 1 and that the terms lion and tiger appear less often than average in document 5. For a matrix of column profiles, a similar interpretation can be made.

### 3 Latent Semantic Analysis

#### 3.1 SVD of Raw Document-Term Matrix

LSA is originally designed for improving information retrieval by using the associations between documents and terms (Deerwester et al., 1990; Dumais et al., 1988). Individual terms provide incomplete and unreliable evidence about the meaning of a document due to synonymy and polysemy. LSA replaces individual terms with derived underlying semantic factors. LSA allows to study the relations between documents, between terms, and between documents and terms.

We start our discussion of LSA with the SVD of a document-term matrix (Berry, Dumais, & O'Brien, 1995; Deisenroth, Faisal, & Ong, 2020). SVD is a mathematical tool that can be used to decompose  $F$  into a product of three matrices:  $U^f$ ,  $\Sigma^f$ , and  $V^f$ , namely

$$F = U^f \Sigma^f (V^f)^T \quad (1)$$

where, assuming  $F$  has size  $m \times n$  and  $n > m$  and  $F$  has full rank,  $U^f$  is a  $m \times m$  matrix with orthonormal columns called left singular vectors, that is,  $(U^f)^T U^f = I$ ,  $V^f$  is a  $n \times m$  matrix with orthonormal columns called right singular vectors, that is,  $(V^f)^T V^f = I$ , and  $\Sigma^f$  is a  $m \times m$  diagonal matrix with singular values on the diagonal in descending order.

We denote the first  $k$  columns of  $U^f$  as the  $m \times k$  matrix  $U_k^f$ , the first  $k$  columns of  $V^f$  as the  $n \times k$  matrix  $V_k^f$ , and the  $k$  largest singular values on the diagonal of  $\Sigma^f$  as the  $k \times k$  matrix  $\Sigma_k^f$  ( $k \leq m$ ). Then  $U_k^f \Sigma_k^f (V_k^f)^T$  provides the optimal rank- $k$  approximation of  $F$  in

a least-squares sense. That is,  $\mathbf{X} = \mathbf{U}_k^f \boldsymbol{\Sigma}_k^f (\mathbf{V}_k^f)^T$  minimizes

$$\|\mathbf{F} - \mathbf{X}\|^2 = \sum_i \sum_j (f_{ij} - x_{ij})^2 \quad (2)$$

amongst all matrices  $\mathbf{X}$  of rank  $k$ . The idea is that the matrix  $\mathbf{U}_k^f \boldsymbol{\Sigma}_k^f (\mathbf{V}_k^f)^T$ , by containing only the first  $k$  independent linear components of  $\mathbf{F}$ , captures the major associational structure in the matrix and throws out noise (Dumais, 1991; Dumais et al., 1988). The total sum of squared singular values is equal to  $\text{tr}((\boldsymbol{\Sigma}^f)^2)$ . The proportion of total sum of squared singular values explained by the rank  $k$  approximation is  $\text{tr}((\boldsymbol{\Sigma}_k^f)^2)/\text{tr}((\boldsymbol{\Sigma}^f)^2)$ .

The SVD can also be interpreted from a geometric point of view. As  $\mathbf{F}$  has size  $m \times n$ , each row of  $\mathbf{F}$  can be represented as point in an  $n$ -dimensional space with the row elements as coordinates. Also, each column of  $\mathbf{F}$  can be represented as point in an  $m$ -dimensional space using the column elements as coordinates. In a rank- $k$  approximation, each of the original  $m$  documents and  $n$  terms are approximated by only  $k$  elements. Also, the SVD projects the sum of squared Euclidean distances from these row (column) points to the origin in the  $n$  ( $m$ )-dimensional space as much as possible to a lower dimensional space. The Euclidean distances between the rows of  $\mathbf{F}$  are approximated by the Euclidean distances between the rows of  $\mathbf{U}_k^f \boldsymbol{\Sigma}_k^f$  from below, and the Euclidean distances between the rows of  $\mathbf{F}^T$  are approximated by the Euclidean distances between the rows of  $\mathbf{V}_k^f \boldsymbol{\Sigma}_k^f$  from below. The choice of  $k$  is crucial to many text mining solutions (Albright, 2004). A lower rank approximation cannot always express prominent relationships in text, whereas the higher rank approximation may add useless noise. How to choose  $k$  is an open issue (Deerwester et al., 1990). In practice, the value of  $k$  is selected such that a certain criterion is satisfied, for example, the proportion of explained total sum of squared singular values is at least a prespecified proportion. Also a scree plot can be considered, see Appendix Figure A1 for examples of scree plots derived from the analysis of the data in the application section.

As it turns out, the raw document-term matrix  $\mathbf{F}$  in Table 1 does not have full rank, its rank is 5. The SVD of  $\mathbf{F}$  in Table 1 is

$$\mathbf{F} = \mathbf{U}^f \boldsymbol{\Sigma}^f (\mathbf{V}^f)^T$$

$$= \begin{bmatrix} -0.411 & 0.175 & 0.825 & 0.252 & -0.239 \\ -0.646 & 0.314 & -0.562 & 0.301 & -0.279 \\ -0.232 & 0.127 & 0.034 & -0.099 & 0.503 \\ -0.562 & -0.203 & 0.044 & -0.603 & 0.333 \\ -0.099 & -0.456 & -0.024 & -0.404 & -0.672 \\ -0.186 & -0.778 & -0.034 & 0.556 & 0.223 \end{bmatrix} \begin{bmatrix} 8.425 & 0 & 0 & 0 & 0 \\ 0 & 3.261 & 0 & 0 & 0 \\ 0 & 0 & 0.988 & 0 & 0 \\ 0 & 0 & 0 & 0.574 & 0 \\ 0 & 0 & 0 & 0 & 0.272 \end{bmatrix} \begin{bmatrix} -0.412 & 0.214 & 0.655 & -0.344 & 0.486 \\ -0.488 & 0.311 & 0.087 & 0.180 & -0.540 \\ -0.440 & 0.257 & -0.748 & -0.259 & 0.339 \\ -0.611 & -0.369 & 0.039 & 0.366 & -0.148 \\ -0.101 & -0.441 & -0.014 & -0.783 & -0.426 \\ -0.123 & -0.679 & -0.048 & 0.186 & 0.392 \end{bmatrix}^T \quad (3)$$

Table 5 shows the singular values, the squares of the singular values, and the proportions of explained total sum of squared singular values (denoted as PSSSV). Together, the

Table 5: The singular values, the squares of singular values, and the proportion of explained total sum of squared singular values (PSSSV) for each dimension of LSA of  $F$ .

	dim1	dim2	dim3	dim4	dim5
singular value	8.425	3.261	0.988	0.574	0.272
square of singular value	70.985	10.635	0.976	0.330	0.074
PSSSV	0.855	0.128	0.012	0.004	0.001

first two dimensions account for  $0.855 + 0.128 = 0.983$  of the total sum of squared singular values. Therefore, the documents and the terms can be approximated adequately in a two dimensional representation using  $U_2^f \Sigma_2^f$  and  $V_2^f \Sigma_2^f$  as coordinates, see Figure 1. As the Euclidean distances between the rows of  $U_2^f \Sigma_2^f$  approximate the Euclidean distances between the rows of  $F$ , the Euclidean distances between the rows of  $F$  can be studied from the Euclidean distances between document points in Figure 1, and similarly for the terms. On the other hand, it is a bit more difficult to study the relation between a document and a term. The reason is that, by choosing both for the documents and for terms a Euclidean distance-representation, the singular values are used twice in the coordinates  $U_2^f \Sigma_2^f$  and  $V_2^f \Sigma_2^f$ , and the inner product of coordinates of a document and coordinates of a term does not approximate the corresponding value in  $F$ . Directions from the origin can be interpreted, though, as the double use of the singular values only leads to relatively reduced coordinates on the second dimension in comparison to the coordinates on the first dimension.

From Figure 1, we see that documents 5 and 6 are close and therefore they appear to be similar. There is an order of 5, 6, 3, 1, 4, and 2 on the first dimension. This order is related to the row margins of Table 1, where 2 and 4 have the highest frequencies and therefore are further away from the origin. Overall the two-dimensional representation of the documents reveals a mix of the row margins and the profiles of terms used by the documents, namely, the row profiles of Table 1. This mix makes the graphic representation difficult to interpret. Similarly, porsche and ferrari are lower left but close to the origin, tiger, cheetah, and lion are upper left and further away from the origin, and jaguar is far away at the lower left. Also here there is a mix of the column margins and the column profiles of Table 1. The directions of the documents and terms away from the origin show that porsche and ferrari are related to documents 5 and 6, tiger, cheetah, and lion to documents 1, 2, and 3, and jaguar to document 4.

Although the first dimension accounts for 85.5% of the total sum of squared singular values, it provides little information about the relations among documents and terms. In particular, from Table 1 we expect that documents 1 to 3 are similar, documents 5 and 6 are similar, and document 4 is in-between; term jaguar is between cat terms (tiger, cheetah, and lion) and car terms (porsche and ferrari), but we cannot see that from the first dimension. This is because the margins of Table 1 play a dominant role in the first dimension.

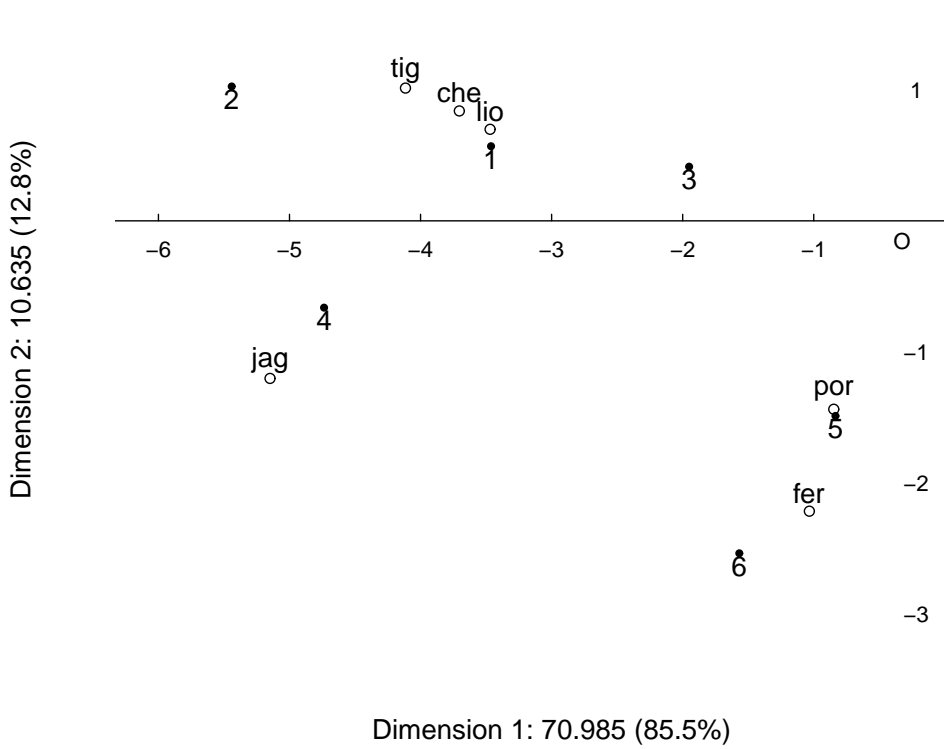


Figure 1: A two-dimensional plot of documents and terms for  $F$ .

### 3.2 SVD of Weighted Document-Term Matrix

Weighting can be used to prevent differential lengths of documents from having differential effects on the representation, or be used to impose certain preconceptions of which terms are more important (Deerwester et al., 1990). The frequencies  $f_{ij}$  in the raw document-term matrix  $F$  can be transformed with the aim to provide a better approximation of the interrelations between documents and terms (Nakov, Popova, & Mateev, 2001). The weight  $w_{ij}$  for term  $j$  in document  $i$  is normally expressed as a product of three components (Ab Samat, Murad, Abdullah, & Atan, 2008; Kolda & O’leary, 1998; Salton & Buckley, 1988)

$$w_{ij} = L(i, j) \times G(j) \times N(i) \quad (4)$$

where the local weighting  $L(i, j)$  is the weight of term  $j$  in document  $i$ , the global weighting  $G(j)$  is the weight of the term  $j$  in the entire document set, and  $N(i)$  is the normalization component for document  $i$ .

When  $L(i, j) = f(i, j)$ ,  $G(j) = 1$ , and  $N(i) = 1$ , the weighted  $F$  is equal to  $F$ . In matrix notation, Equation (4) can be expressed as  $W = NLG$ , where  $N$  is a diagonal matrix with diagonal elements  $N(i)$  and  $G$  is a diagonal matrix with diagonal elements  $G(j)$ . Notice that pre- or post-multiplying by a diagonal matrix leaves the rank of the matrix  $L$  intact.

We present two ways to weight  $f_{ij}$ . One is row normalization. The other is term

frequency-inverse document frequency model.

### 3.2.1 SVD of Matrix with Row-Normalized Elements

In row-normalized weighting, we use Equation (4) with  $L(i, j) = f_{ij}$ ,  $G(j) = 1$ , and  $N(i) = 1/\sqrt{\sum_{j=1}^n f_{ij}^2}$  (Ab Samat et al., 2008; Salton & Buckley, 1988), and apply an SVD to this transformed matrix that we denote as  $F^N$ , see Table 6.

Table 6: A document-term matrix  $F^N$

	lion	tiger	cheetah	jaguar	porsche	ferrari
doc1	0.555	0.555	0.277	0.555	0.000	0.000
doc2	0.359	0.539	0.539	0.539	0.000	0.000
doc3	0.500	0.500	0.500	0.500	0.000	0.000
doc4	0.417	0.417	0.417	0.626	0.209	0.209
doc5	0.000	0.000	0.000	0.577	0.577	0.577
doc6	0.000	0.000	0.000	0.667	0.333	0.667

Table 7: The singular value, the squares of singular values, and the proportion of explained total sum of squared singular values (PSSSV) for each dimension of LSA of  $F^N$ .

	dim1	dim2	dim3	dim4	dim5
singular value	2.095	1.228	0.239	0.198	0.092
square of singular value	4.388	1.507	0.057	0.039	0.009
PSSSV	0.731	0.251	0.009	0.007	0.001

We perform LSA of Table 6 and find Table 7. This shows that a rank 2 matrix approximates the data well as  $0.731 + 0.251 = 0.982$  of the total sum of squared singular values is explained by these two dimensions. The first two columns of LSA of  $F^N$  can be used to approximate  $F^N$ , see Equation (5).

$$\begin{aligned}
 F^N &\approx U_2^N \Sigma_2^N (V_2^N)^T \\
 &= \begin{bmatrix} -0.443 & 0.259 \\ -0.445 & 0.271 \\ -0.444 & 0.295 \\ -0.476 & 0.017 \\ -0.293 & -0.635 \\ -0.310 & -0.608 \end{bmatrix} \begin{bmatrix} 2.095 & 0 \\ 0 & 1.228 \end{bmatrix} \begin{bmatrix} -0.394 & 0.323 \\ -0.432 & 0.362 \\ -0.374 & 0.304 \\ -0.659 & -0.263 \\ -0.178 & -0.460 \\ -0.227 & -0.625 \end{bmatrix}^T \quad (5)
 \end{aligned}$$

Documents and terms can be projected on a two dimensional space using  $U_2^N \Sigma_2^N$  and  $V_2^N \Sigma_2^N$  as coordinates, see Figure 2. In this representation documents 1, 2, and 3 are quite close, and so are 5 and 6. Also, the terms ferrari and porsche are close and related to 5 and 6, tiger, lion, and cheetah are close and related to 1, 2, and 3.

Although the first dimension accounts for 73.1% of the total sum of squared singular values, we do not find document 4 in between documents 1-3 on the one hand and documents 5-6 on the other hand on this dimension. This is caused by the high values in the



row for doc4 in Table 6, which lead to a larger distance from the origin. Also, we would expect jaguar to be in between cat terms (tiger, cheetah, and lion) and car terms (porsche and ferrari), but on the first dimension it appears as a separate, third group. This is caused by the high values in its column in Table 6, which lead to a larger distance from the origin.

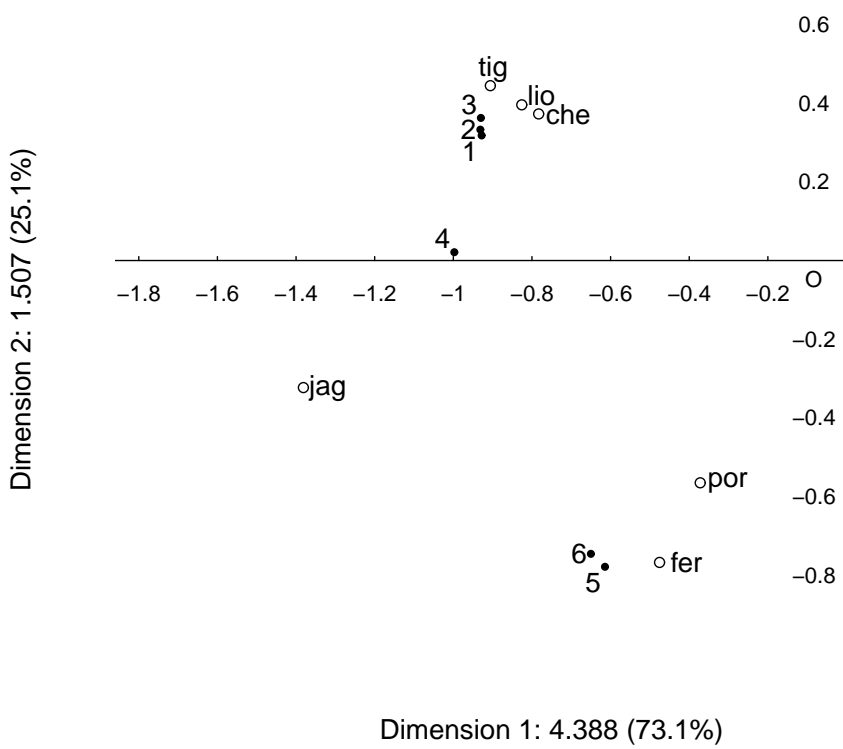


Figure 2: A two-dimensional plot of documents and terms for row-normalized data  $F^N$ .

### 3.2.2 SVD of the Term Frequency-Inverse Document Frequency Matrix

Table 8: A document-term matrix  $F^{\text{TF-IDF}}$

	lion	tiger	cheetah	jaguar	porsche	ferrari
doc1	3.170	3.170	1.585	2	0	0
doc2	3.170	4.755	4.755	3	0	0
doc3	1.585	1.585	1.585	1	0	0
doc4	3.170	3.170	3.170	3	2	2
doc5	0.000	0.000	0.000	1	2	2
doc6	0.000	0.000	0.000	2	2	4

The term frequency-inverse document frequency (TF-IDF) is one commonly used vector space representation of text data. We use Equation (4) with  $L(i, j) = f_{ij}$ ,  $G(j) = 1 + \log(\frac{n_{\text{docs}}}{df_j})$ , and  $N(i) = 1$ , one form of TF-IDF, where  $n_{\text{docs}}$  is the number of documents in the set and  $df_j$  is the number of documents where term  $j$  appears (Dumais, 1991),

and then apply an SVD to this transformed matrix that we denote as  $F^{\text{TF-IDF}}$ , see Table 8. Here we choose the base of the logarithmic function to be equal to 2.

Table 9: The singular value, the squares of singular values, and the proportion of explained total sum of squared singular values (PSSSV) for each dimension of LSA of  $F^{\text{TF-IDF}}$ .

	dim1	dim2	dim3	dim4	dim5
singular value	11.878	5.898	1.565	1.017	0.449
square of singular value	141.088	34.782	2.451	1.034	0.202
PSSSV	0.786	0.194	0.014	0.006	0.001

We perform LSA of Table 8 and find Table 9. This shows that a rank 2 matrix approximates the data well as  $0.786 + 0.194 = 0.980$  of the total sum of squared singular values is explained by these two dimensions. The matrix  $F^{\text{TF-IDF}}$  in Table 8 is approximated in the first two dimensions as follows:

$$\begin{aligned}
 F^{\text{TF-IDF}} &\approx U_2^{\text{TF-IDF}} \Sigma_2^{\text{TF-IDF}} (V_2^{\text{TF-IDF}})^T \\
 &= \begin{bmatrix} -0.411 & 0.175 \\ -0.654 & 0.296 \\ -0.239 & 0.112 \\ -0.563 & -0.245 \\ -0.086 & -0.469 \\ -0.148 & -0.768 \end{bmatrix} \begin{bmatrix} 11.878 & 0 \\ 0 & 5.898 \end{bmatrix} \begin{bmatrix} -0.466 & 0.151 \\ -0.554 & 0.231 \\ -0.499 & 0.184 \\ -0.429 & -0.236 \\ -0.134 & -0.502 \\ -0.159 & -0.763 \end{bmatrix}^T \quad (6)
 \end{aligned}$$

Figure 3 is a two-dimensional plot of the documents and terms using  $U_2^{\text{TF-IDF}} \Sigma_2^{\text{TF-IDF}}$  and  $V_2^{\text{TF-IDF}} \Sigma_2^{\text{TF-IDF}}$  as coordinates for the  $6 \times 6$  sample document-term matrix  $F^{\text{TF-IDF}}$ . The configuration of documents in Figure 3 is very similar to that in Figure 1. The configuration of terms in Figure 3 is different from that of terms in Figure 1. In Figure 3, there is an order of porsche, ferrari, jaguar, lion, cheetah, and tiger on the first dimension, whereas in Figure 1, there is an order of porsche, ferrari, lion, cheetah, tiger, and jaguar on the first dimension. Compared with Figure 1, the first dimension of Figure 3 shows that jaguar is in between cat terms (tiger, cheetah, and lion) and car terms (porsche and ferrari).

### 3.3 Conclusion about LSA of Different Matrices

We conclude that normalization of the documents has a beneficial effect. Yet, the properties of the frequencies that are evident from the Table 1 where we expect, for example, that jaguar lies in between porsche and ferrari on the one hand and tiger, cheetah, and lion on the other hand, are not fully represented on the first dimension. This is due to the fact that the column margins of Table 6 still play a role on the first dimension. The TF-IDF matrix also has a positive effect. Yet, it is not successful, for example, in representing the expected relationships between documents on the first dimension that documents 1 to 3 are similar, 5 and 6 are similar, and document 4 is in-between. This is due to the fact that the row margins of Table 8 still play a role on the first dimension. We can try to repair this aspect

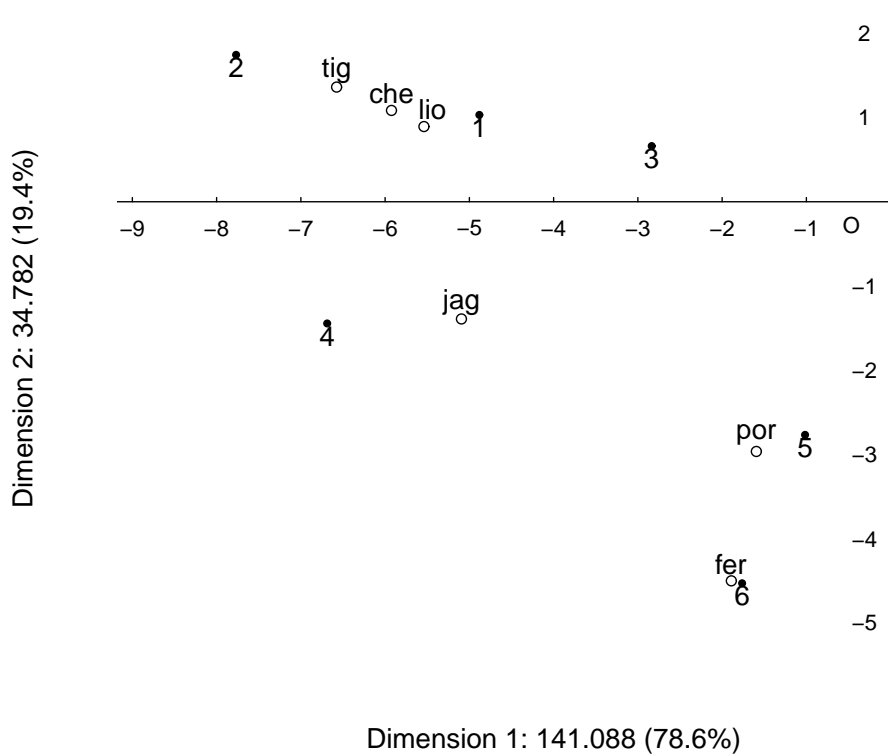


Figure 3: A two-dimensional plot of documents and terms for matrix  $F^{\text{TF-IDF}}$ .

as well, by applying a transformation of the rows and columns of Table 1 simultaneously. However, the transformations appear a bit ad hoc. Instead we present in the next section a different technique, which better fits the properties of the data: CA.

## 4 Correspondence Analysis

CA provides a low-dimensional representation of the interaction or dependence between the rows and columns of the contingency table (Greenacre & Hastie, 1987), which can be used to reveal the structure in the data (Hayashi, 1992). CA is proposed multiple times, apparently independently, emphasizing different properties of the technique. Some important contributions are provided in the Japanese literature, by Hayashi (1956, 1992), who emphasizes the property of CA that it maximizes the correlation coefficient between the row and column variable by assigning numerical scores to these variables; in the French literature, by Benzécri (1973), who emphasize a distance interpretation, where Greenacre (1984) expressed Benzécri’s work in a more convenient mathematical notation; and in the Dutch literature, by Gifi (1990); Michailidis and De Leeuw (1998), who emphasize optimal scaling properties. We present CA here mainly from the French perspective.

The aim of CA as developed by Benzécri is to find a representation of the rows of frequency matrix  $F$  in such a way that Euclidean distances between the rows correspond

to so-called  $\chi^2$ -distances between rows of  $\mathbf{F}$  (Gifi, 1990). As in Section 2, we work with  $\mathbf{P}$  with elements  $p_{ij} = f_{ij}/\sum_i \sum_j f_{ij}$ . In the  $\chi^2$ -distance profiles play an important role. The squared  $\chi^2$ -distance between the  $k$ th row profile with elements  $p_{kj}/r_k$  and the  $l$ th row profile with elements  $p_{lj}/r_l$  is

$$\delta_{kl}^2 = \sum_j \frac{(p_{kj}/r_k - p_{lj}/r_l)^2}{c_j} \quad (7)$$

Thus the difference between the  $j$ th elements of the two profiles is weighted by column margin of Table 2,  $c_j$ , so that this difference plays a relatively more important role in the  $\chi^2$ -distance if it stems from a column having a small value  $c_j$ .

A graphic representation where Euclidean distances between the rows of the matrix are equal to  $\chi^2$ -distances is found as follows. In matrix notation, the matrix whose Euclidean distances between the rows are equal to  $\chi^2$ -distances between rows of  $\mathbf{F}$  is equal to  $\mathbf{D}_r^{-1} \mathbf{P} \mathbf{D}_c^{-\frac{1}{2}}$ , where  $\mathbf{D}_r$  is a diagonal matrix with  $r_i$  as diagonal elements and  $\mathbf{D}_c$  is a diagonal matrix with  $c_j$  as diagonal elements. Suppose we take the SVD of

$$\mathbf{D}_r^{-\frac{1}{2}} \mathbf{P} \mathbf{D}_c^{-\frac{1}{2}} = \mathbf{U}^{sp} \mathbf{\Sigma}^{sp} (\mathbf{V}^{sp})^T \quad (8)$$

Here  $\mathbf{D}_r^{-\frac{1}{2}} \mathbf{P} \mathbf{D}_c^{-\frac{1}{2}}$  is a matrix with standardized proportions, hence the superscripts sp on the right hand side of the equation. Then, if we pre-multiply both sides of the Equation (8) with  $\mathbf{D}_r^{-\frac{1}{2}}$ , we get:

$$\mathbf{D}_r^{-1} \mathbf{P} \mathbf{D}_c^{-\frac{1}{2}} = \mathbf{D}_r^{-\frac{1}{2}} \mathbf{U}^{sp} \mathbf{\Sigma}^{sp} (\mathbf{V}^{sp})^T \quad (9)$$

Thus a graphic representation using the rows of  $\mathbf{D}_r^{-\frac{1}{2}} \mathbf{U}^{sp} \mathbf{\Sigma}^{sp}$  as row coordinates leads to Euclidean distances between these row points being equal to  $\chi^2$ -distances between rows of  $\mathbf{F}$ . Similar to Equation (7) we can also define  $\chi^2$ -distances between the columns of  $\mathbf{F}$ , and in matrix notation this leads to the matrix  $\mathbf{D}_r^{-\frac{1}{2}} \mathbf{P} \mathbf{D}_c^{-1}$ . Then, in a similar way as for the  $\chi^2$ -distances for the rows, Equation (8) can be used as an intermediate step to go to a solution for the columns. Post-multiplying the left hand and right hand side in Equation (8) by  $\mathbf{D}_c^{-\frac{1}{2}}$  provides us with the coordinates for a graphic representation where Euclidean distances between the column points (the rows of  $\mathbf{D}_c^{-\frac{1}{2}} \mathbf{V}^{sp} \mathbf{\Sigma}^{sp}$  as coordinates for these columns) are equal to  $\chi^2$ -distances between the columns of  $\mathbf{F}$ . Notice that Equation (8) plays the dual role of an intermediate step in going to a solution both for the rows and the columns.

The matrices  $\mathbf{D}_r^{-\frac{1}{2}} \mathbf{U}^{sp} \mathbf{\Sigma}^{sp}$  and  $\mathbf{D}_c^{-\frac{1}{2}} \mathbf{V}^{sp} \mathbf{\Sigma}^{sp}$  have a first column being equal to 1, a so-called artificial dimension. This artificial dimension reflects the fact that the row margins of the matrix  $\mathbf{D}_r^{-1} \mathbf{P}$  with the row profiles of Table 1 are 1 and the column margins of the matrix  $\mathbf{P} \mathbf{D}_c^{-1}$  with the column profiles of Table 1 are 1. This artificial dimension is eliminated by not taking the SVD of  $\mathbf{D}_r^{-\frac{1}{2}} \mathbf{P} \mathbf{D}_c^{-\frac{1}{2}}$  but of  $\mathbf{D}_r^{-\frac{1}{2}} (\mathbf{P} - \mathbf{E}) \mathbf{D}_c^{-\frac{1}{2}}$ , where the elements of  $\mathbf{E}$  are defined in Table 3 as the product of the margins  $r_i$  and  $c_j$ . Due to subtracting  $\mathbf{E}$  from  $\mathbf{P}$ , the rank of  $\mathbf{D}_r^{-\frac{1}{2}} (\mathbf{P} - \mathbf{E}) \mathbf{D}_c^{-\frac{1}{2}}$  is  $m - 1$ , which is 1 less than the rank of  $\mathbf{F}$ . Notice that the elements of  $\mathbf{D}_r^{-\frac{1}{2}} (\mathbf{P} - \mathbf{E}) \mathbf{D}_c^{-\frac{1}{2}}$  are standardized residuals under the independence

model, and the sum of squares of these elements yields the so-called total inertia. By taking the SVD of the matrix of standardized residuals, we get

$$D_r^{-\frac{1}{2}}(P - E)D_c^{-\frac{1}{2}} = U^{sr}\Sigma^{sr}(V^{sr})^T \quad (10)$$

and

$$D_r^{-1}(P - E)D_c^{-1} = \Phi^{sr}\Sigma^{sr}(\Gamma^{sr})^T \quad (11)$$

where  $\Phi^{sr} = D_r^{-\frac{1}{2}}U^{sr}$  and  $\Gamma^{sr} = D_c^{-\frac{1}{2}}V^{sr}$ . We use the abbreviation sr for the matrices on the right hand side of Equation (10) to refer to the matrix of standardized residuals on the left hand side of the equation. CA simultaneously provides a geometric representation of row profiles and column profiles of Table 1, where the effects of row margins and column margins of Table 1 are eliminated.  $\Phi^{sr}$  and  $\Gamma^{sr}$  are called standard coordinates of rows and columns respectively. They have the property that their weighted average is 0 and weighted sum of squares is 1:

$$\mathbf{1}^T D_r \Phi^{sr} = \mathbf{0}^T = \mathbf{1}^T D_c \Gamma^{sr} \quad (12)$$

and

$$(\Phi^{sr})^T D_r \Phi^{sr} = \mathbf{I} = (\Gamma^{sr})^T D_c \Gamma^{sr} \quad (13)$$

Equation (12) reflects the fact that the row and column margins of  $P - E$  vanish (Van der Heijden, De Falguerolles, & De Leeuw, 1989).

We can make graphic displays using  $\Phi_k^{sr}\Sigma_k^{sr}$  and  $\Gamma_k^{sr}\Sigma_k^{sr}$  as coordinates, which has the advantage that Euclidean distances between the points approximate  $\chi^2$ -distances both for the rows of  $F$  and for the columns of  $F$ , but it has the drawback that  $\Sigma_k^{sr}$  is used twice. We can also make graphic displays using  $\Phi_k^{sr}\Sigma_k^{sr}$  and  $\Gamma_k^{sr}$ , or  $\Phi_k^{sr}$  and  $\Gamma_k^{sr}\Sigma_k^{sr}$ . Thus, from Equation (11), this has the advantage that the inner product of the coordinates of a document and the coordinates of a term approximates the corresponding value in  $D_r^{-1}(P - E)D_c^{-1}$ .

If we choose  $\Phi^{sr}\Sigma^{sr}$  for the row points and  $\Gamma^{sr}$  for the column points, then CA has the property that the row points are in weighted average of the column points, where the weights are the row profile values. Actually,  $\Gamma^{sr}$  can be seen as coordinates for the extreme row profiles projected onto the subspace. The extreme row profiles are totally concentrated into one of the terms. For example,  $[0, 0, 1, 0, 0, 0]$  represents the row profile of a document that is totally concentrated into cheetah. At the same time, if we choose  $\Phi^{sr}$  for the row points and  $\Gamma^{sr}\Sigma^{sr}$  for the column points, column points are in weighted average of row points, where the weights are the column profile values. In a similar way as for the rows,  $\Phi^{sr}$  provide coordinates for the extreme column profiles projected onto the subspace. The relationship between these row points and column points can be shown by rewriting Equation (10) and using Equation (12) as

$$D_r^{-1}P\Gamma^{sr} = \Phi^{sr}\Sigma^{sr} \quad (14)$$

and

$$D_c^{-1} P^T \Phi^{sr} = \Gamma^{sr} \Sigma^{sr} \quad (15)$$

These equations are called the transition formulas. In fact, this is one of the ways in which the solution of CA can be obtained: starting from arbitrary values for the columns, one first centers and standardizes the column coordinates so that the weighted sum is 0 and the weighted sums of squares is 1, next places the rows in the weighted average of the columns, then places the columns in the weighted average of the rows, and so on, until convergence. This is known as reciprocal averaging (Hill, 1973, 1974).

The origin in the graphic representation for the rows stands for average row profile, which can be seen as follows. Let  $D_r^{-1} P D_c^{-\frac{1}{2}}$  be the matrix where Euclidean distances between the rows are  $\chi^2$ -distances between rows of  $F$ . Assume we plot the rows of this matrix using the  $n$  elements of each row as coordinates. Then, eliminating the artificial dimension in  $D_r^{-1} P D_c^{-\frac{1}{2}}$  leads to the subtraction of the average row profile from each row, as  $D_r^{-1} E$  is a matrix with the average row profile in each row. In other words, the cloud of row points is translated to the origin, with the average row profile being exactly in the origin (compare Equation (12):  $0^T = \mathbf{1}^T D_c \Gamma^{sr}$ ). When two row points are departing in the same way from the origin, they depart in the same way from the average profile, and when two row points are on opposite sides of the origin, they depart in opposite ways from the average profile. If the documents and terms are statistically independent, then  $p_{ij}/r_i = c_j$ , and all document profiles would lie in the origin. Thus comparing row profiles with the origin is a way to study the departure from independence and to study the relations between documents and terms (see Section 2). Similarly, the origin in the graphic representation for the columns stands for average column profile.

We now analyse the example discussed in the LSA section. Table 10 shows the matrix  $D_r^{-\frac{1}{2}}(P - E)D_c^{-\frac{1}{2}}$  of standardized residuals (in lower-case notation, the elements of the matrix are  $(p_{ij} - e_{ij})/\sqrt{e_{ij}}$ ).

Table 10: The matrix  $D_r^{-\frac{1}{2}}(P - E)D_c^{-\frac{1}{2}}$  of standardized residuals

	lion	tiger	cheetah	jaguar	porsche	ferrari
doc1	0.115	0.085	-0.028	-0.005	-0.112	-0.129
doc2	0.014	0.091	0.128	-0.019	-0.140	-0.162
doc3	0.060	0.039	0.060	-0.025	-0.084	-0.098
doc4	0.014	-0.016	0.014	-0.019	0.034	-0.011
doc5	-0.112	-0.119	-0.112	0.020	0.260	0.204
doc6	-0.144	-0.154	-0.144	0.069	0.164	0.338

We perform an SVD of  $D_r^{-\frac{1}{2}}(P - E)D_c^{-\frac{1}{2}}$  in Table 10 and find Table 11. Due to subtracting  $E$  from  $P$ , the rank of the matrix in Table 10 is 4, which is 1 less than that in Table 1. The proportion of the total inertia explained by only the first dimension accounts for 0.932 of the total inertia. The matrix  $D_r^{-\frac{1}{2}}(P - E)D_c^{-\frac{1}{2}}$  in Table 10 is approximated in the first

Table 11: The singular values, the inertia, and the proportions of explained total inertia for each dimension of CA.

	dim1	dim2	dim3	dim4
singular value	0.689	0.131	0.124	0.044
inertia	0.475	0.017	0.015	0.002
the proportion of inertia	0.932	0.034	0.030	0.004

two dimensions as follows:

$$D_r^{-\frac{1}{2}}(P - E)D_c^{-\frac{1}{2}} \approx U_2^{sr} \Sigma_2^{sr} (V_2^{sr})^T$$

$$= \begin{bmatrix} -0.286 & 0.789 \\ -0.368 & -0.517 \\ -0.231 & -0.025 \\ 0.007 & -0.138 \\ 0.547 & -0.206 \\ 0.656 & 0.220 \end{bmatrix} \begin{bmatrix} 0.689 & 0 \\ 0 & 0.131 \end{bmatrix} \begin{bmatrix} -0.301 & 0.544 \\ -0.338 & 0.090 \\ -0.303 & -0.761 \\ 0.102 & 0.152 \\ 0.512 & -0.275 \\ 0.656 & 0.136 \end{bmatrix}^T \quad (16)$$

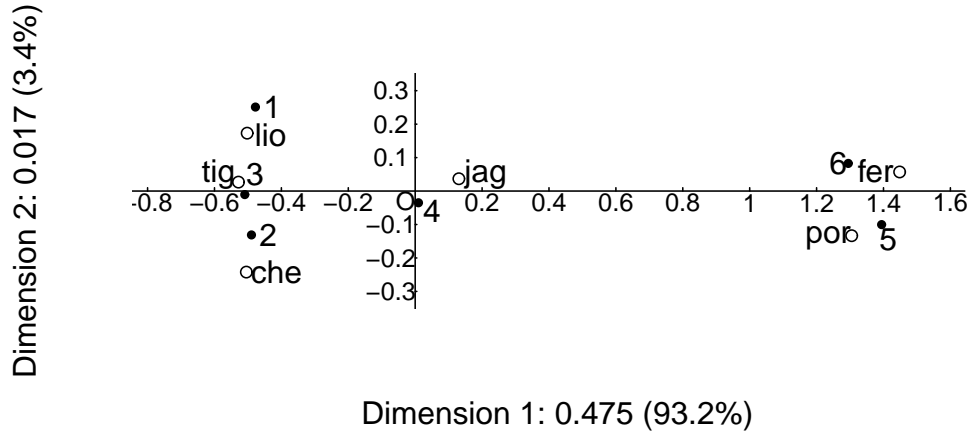


Figure 4: Symmetric map of the data of Table 1.

Figure 4 is the map with a symmetric role for the rows and the columns, having  $\Phi_2^{sr} \Sigma_2^{sr}$  and  $\Gamma_2^{sr} \Sigma_2^{sr}$  as coordinates. The larger deviations from document (term) points to the origin are, the larger the dependence between documents and terms. Looking only at the first dimension and document profiles' positions, we can see that the groups furthest apart are documents 1-3 on the left-hand side, opposed to documents 5-6 on the right-hand side. They differ in opposite ways from the average row profile that lies in the origin. Document 4 lies between documents 1-3 and documents 5-6. For the term points on the first dimension, cat terms (tiger, cheetah, and lion) lie on the left and car terms (porsche and ferrari) on the right. They differ in opposite ways from the average column profile. Jaguar lies between cat terms and car terms.

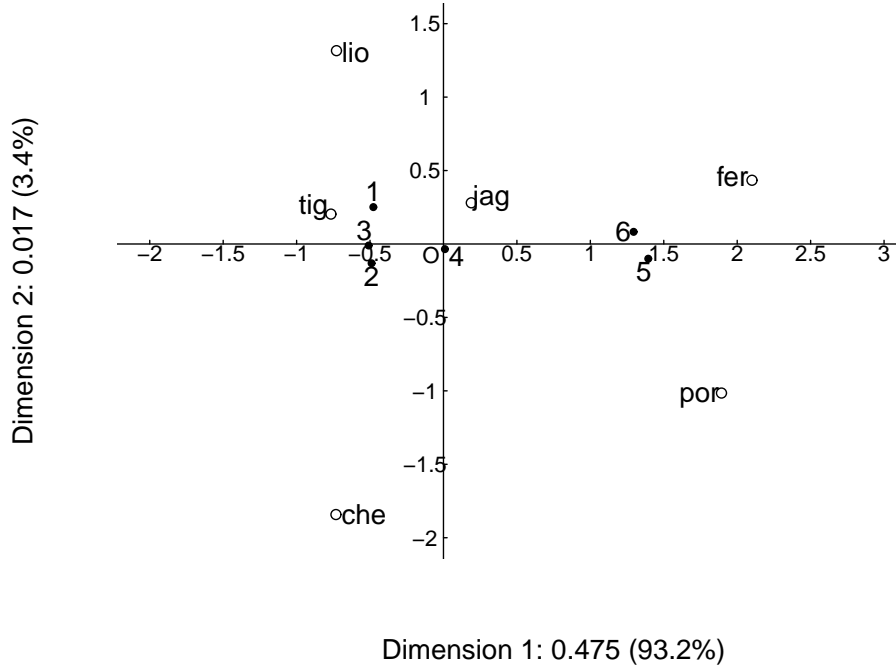


Figure 5: Asymmetric map of the data of Table 1.

Figure 5 is the asymmetric map with documents in the weighted average of the terms ( $\Phi_2^{sr}$   $\Sigma_2^{sr}$  and  $\Gamma_2^{sr}$  as coordinates, notice that the position of the documents is identical as in Figure 4). From this graphic display we can study the position of the documents as they are in the weighted average of the terms, using the row profile elements as weights. For example, document 1 is closer to lion and tiger than to porsche and ferrari, because it has higher profile values than average values on terms lion and tiger (both 0.286 in comparison with the average profile values 0.171 and 0.195) and lower profile values on the terms porsche and ferrari (both 0.000 in comparison to 0.073 and 0.098), see Table 4. Thus document 1 is pulled into the direction of lion and tiger.

CA is related to statistical models in the following way. First, the SVD is taken from the matrix of standardized residuals under the independence model, in lower case  $(p_{ij} - r_i c_j) / (r_i c_j)^{1/2}$ . As a result of this, the squared sum of the singular values is equal to the Pearson  $\chi^2$  statistic divided by sample size  $\sum_i \sum_j f_{ij}$ , also known as Pearson's index of mean-square contingency. This illustrates that CA provides a decomposition of the departure of the statistical independence model, a property of CA that was emphasized in the work of Van der Heijden et al. (1989).

Second, using Equation (11) we can write CA as a decomposition for the elements  $p_{ij}$  as

$$p_{ij} = r_i c_j \left( 1 + \sum_{k=1}^{\text{rank}(P)-1} \delta_k^{sr} \phi_{ik}^{sr} \gamma_{jk}^{sr} \right) \quad (17)$$



which is also called the reconstitution formula (Greenacre, 1984). This model-like formulation illustrates again that in CA the departure from statistical independence  $r_i c_j$  is decomposed into a number of dimensions. Equation (17) reconstitutes the matrix  $\mathbf{P}$  from the matrices  $\Phi^{sr}$ ,  $\Sigma^{sr}$ , and  $\Gamma^{sr}$ . A rank  $K + 1$  approximation of  $\mathbf{P}$  using the submatrices  $\Phi_K^{sr}$ ,  $\Sigma_K^{sr}$ , and  $\Gamma_K^{sr}$  is

$$\pi_{ij}^{sr} = r_i c_j \left( 1 + \sum_{k=1}^K \delta_k^{sr} \phi_{ik}^{sr} \gamma_{jk}^{sr} \right) \quad (18)$$

This inspired Goodman (1985) and Gilula and Haberman (1986) to propose CA as a model using a lower-rank than  $m - 1$  estimated by maximum likelihood.

Last, it is well known that CA is related to canonical correlation analysis of two categorical variables (Greenacre, 2017). Consider the group of the  $m$  documents and group of  $n$  terms as categorical variables. If the  $m$  categories of the document variable and the  $n$  categories of the term variable would have been assigned scores, then a correlation coefficient between these two variables can be calculated. When we use the coordinate values of the documents and terms on the first axis of CA for this, for example,  $\Phi_1^{sr}$  and  $\Gamma_1^{sr}$ , the correlation coefficient is maximized over all possible scorings, and is equal to the first singular value.

## 5 A Unifying Framework

From the analysis of Section 4, we can see that, weighting  $\mathbf{F}$ , subtracting the matrix related to the row or column margins of  $\mathbf{F}$ , and weighting the documents or terms after SVD are all methods to weight documents and terms. In CA, these three mechanisms are used: weighting  $\mathbf{F}$  with  $\mathbf{D}_r^{-\frac{1}{2}} \mathbf{P} \mathbf{D}_c^{-\frac{1}{2}}$ ; subtracting  $\mathbf{r}^{\frac{1}{2}} (\mathbf{c}^{\frac{1}{2}})^T$ ; weighting the documents after SVD by  $\mathbf{D}_r^{-\frac{1}{2}}$  and weighting the terms after SVD by  $\mathbf{D}_c^{-\frac{1}{2}}$ . However, in LSA, researchers usually use one mechanism: weighting  $\mathbf{F}$ , where the matrix subtracted is  $\mathbf{0}$ . We put forth a unifying framework that includes these three mechanisms. The weight  $a_{ij}$  for term  $j$  in document  $i$  is:

$$a_{ij} = (L(i, j) \times G(j) - R(i) \times C(j)) \times N(i) \quad (19)$$

where  $L(i, j)$ ,  $G(j)$ , and  $N(i)$  have the same meaning as in Equation (4),  $R(i)$  and  $C(j)$  are related to margins of document and term respectively. In matrix notation, Equation (19) is expressed as  $\mathbf{A} = \mathbf{N} (\mathbf{L}\mathbf{G} - \mathbf{R}\mathbf{C})$ . Its SVD is

$$\mathbf{A} = \mathbf{U}^a \mathbf{\Sigma}^a (\mathbf{V}^a)^T \quad (20)$$

The rows of  $\mathbf{M}\mathbf{U}_k^a \mathbf{\Sigma}_k^a$  provide coordinates of documents in  $k$ -dimensional subspace and the rows of  $\mathbf{H}\mathbf{V}_k^a \mathbf{\Sigma}_k^a$  provide coordinates of terms in  $k$ -dimensional subspace, where  $\mathbf{M}$  and  $\mathbf{H}$  are diagonal matrices whose diagonal elements  $M(i)$  and  $H(j)$  weight documents and terms respectively.

Murtagh et al. (2016) pointed out CA is a LSA method just like the TF-IDF transformation, but CA does not fit into Equation (4) due to the subtraction of  $\mathbf{r}^{\frac{1}{2}} (\mathbf{c}^{\frac{1}{2}})^T$ . Our

framework unifies LSA and CA. For example, the unifying framework with  $L(i, j) = f_{ij}$ ,  $G(j) = 1 + \log(\frac{n_{docs}}{df_j})$ ,  $R(i) = 0$  or  $C(j) = 0$ ,  $N(i) = 1$ ,  $M(i) = 1$ , and  $H(j) = 1$  degenerates to the TF-IDF transformation introduced in Section 3.2.2. CA can be obtained by the unifying framework with  $L(i, j) = \frac{f_{ij}}{\sqrt{\sum_j f_{ij}}}$ ,  $G(j) = \frac{1}{\sqrt{\sum_i f_{ij}}}$ ,  $R(i) = \sqrt{\frac{\sum_j f_{ij}}{\sum_i \sum_j f_{ij}}}$ ,  $C(j) = \sqrt{\frac{\sum_i f_{ij}}{\sum_i \sum_j f_{ij}}}$ ,  $N(i) = 1$ ,  $M(i) = \sqrt{\frac{\sum_i \sum_j f_{ij}}{\sum_j f_{ij}}}$ , and  $H(j) = \sqrt{\frac{\sum_i \sum_j f_{ij}}{\sum_i f_{ij}}}$ .

## 6 Authorship Attribution of the *Wilhelmus*

Authorship attribution is the process of identifying the authorship of a document and its applications include plagiarism detection and authorship disputes (Bozkurt, Baghoglu, & Uyar, 2007). The *Wilhelmus* is the national anthem of the Netherlands and its author is unknown. Although there is a substantive amount of qualitative research attempting to determine the authorship of the *Wilhelmus*, to the best of our knowledge, the authorship of the *Wilhelmus* was first studied by statistical methods and computational means in Winkel (2015). After that, Kestemont et al. (2017a, 2017b) studied the question by PCA and the General Imposters (GI) method. Vargas Quiros (2017) used the KRIMP compression algorithm and Kullback-Leibler Divergence to study the author of the *Wilhelmus*.

The LSA and CA have been used for authorship attribution before. For example, Soboroff, Nicholas, Kukla, and Ebert (1997) applied LSA with n-grams as terms to visualize authorship among biblical Hebrew texts. McCarthy, Lewis, Dufty, and McNamara (2006) applied LSA to lexical features to automatically detect semantic similarities between words (Stamatatos, 2009). Satyam, Dawn, and Saha (2014) used LSA on a character n-gram based representation to build a similarity measure between a questioned document and known documents. Mealand (1995) studied the Gospel of Luke using a visualization provided by CA. Mealand (1997) also measured genre differences in Mark by CA. Mannion and Dixon (2004) applied CA to study authorship attribution of the case of Oliver Goldsmith by visualization.

In this section, we will investigate who of the contemporary writers wrote in a way similar to the author of the *Wilhelmus*, with the aim to assign the authorship to one of them (Kestemont et al., 2017a, 2017b). We use 186 documents of these contemporary writers, consisting of 35 documents written by Datheen, 46 documents written by Marnix, 23 documents written by Heere, 35 documents written by Haecht, 33 documents written by Fruytiers, and 14 documents written by Coornhert, which was made publicly available by Kestemont, Stover, Koppel, Karsdorp, and Daelemans (2016); Kestemont et al. (2017a, 2017b). They use tag-lemma pairs, obtained through part-of-speech tagging and lemmatizing of the texts, as terms.

We use two methods based on LSA and CA to study the authorship of the *Wilhelmus*. One is visualization, where we use LSA and CA to visualize documents by projecting them onto two dimensions. The other is to apply LSA and CA together with distance measures. In line with the foregoing sections, we denote the raw document-term matrix by  $F$ . For

LSA we study three versions: LSA of  $F$  (LSARAW), LSA of the row-normalized matrix  $F^N$  (LSANROW), and LSA of the TF-IDF matrix  $F^{\text{TF-IDF}}$  (LSATFIDF). We also directly perform distance measures on the raw document-term matrix, denoted as RAW, where no dimensionality reduction has taken place, used for performance comparison.

## 6.1 Visualization

In this section, we investigate authorship of the *Wilhelmus* by visualizations. First, we explore all documents of the authors Datheen and Marnix, and the *Wilhelmus* that form a document-term matrix of size  $82 \times 300$  (the 300 most frequent tag-lemma pairs). Figure 6 illustrates the results of an analysis of this document-term matrix by LSARAW, LSANROW, LSATFIDF, and CA. Although the first 2 dimensions for CA ( $11.2\% + 8.6\% = 19.8\%$ ) account for a much smaller percentage of the total sum of squared singular values than the first 2 dimensions for LSARAW ( $67.6\% + 12.2\% = 79.8\%$ ), LSANROW ( $67.8\% + 11.7\% = 79.5\%$ ), and LSATFIDF ( $53.8\% + 11.1\% = 64.9\%$ ), CA can separate documents from authors Datheen and Marnix well and the *Wilhelmus* is attributed to Datheen, whereas LSARAW, LSANROW, and LSATFIDF cannot separate documents from authors Datheen and Marnix. This is because the margins play an important role in the first two dimension for LSARAW, LSANROW, and LSATFIDF and the relations between documents are blurred by these margins.

Given the effectiveness of CA and the attribution of the *Wilhelmus* to Datheen in the above analysis, we apply CA to all documents of two candidate authors including Datheen, and the *Wilhelmus*, see Figure 7. CA can separate documents from author Datheen and each other author well except for Haecht.

Finally, we explore all documents of the six authors, and the *Wilhelmus*, which form a document-term matrix of size  $187 \times 300$ . Figure 8 shows the results of the analysis of this matrix by LSARAW, LSANROW, LSATFIDF, and CA. The LSA methods cannot separate the authors of our dataset well, but CA does a reasonably good job. Again we find that, although the percentage of the total sum of squared singular values in the first two dimensions for CA ( $8.6\% + 5.7\% = 14.3\%$ ) is lower than LSARAW ( $64.1\% + 11.1\% = 75.2\%$ ), LSANROW ( $64.1\% + 10.0\% = 74.1\%$ ), and LSATFIDF ( $48.7\% + 10.5\% = 59.2\%$ ), CA separates the documents written by Marnix effectively from the documents written by other authors.

## 6.2 Distance Measures

In this section, we use distance measures to study the authorship of the *Wilhelmus*. The idea is simple: the *Wilhelmus* is attributed to the author, whose distance from the *Wilhelmus* to all documents of this author is smallest among all authors. We test four different methods for measuring the distance from a document to a set of documents (Guthrie, 2008; Kestemont et al., 2016; Koppel & Seidman, 2013). One method is to obtain the distance by calculating the Euclidean distance between the document and the centroid of the set of documents (denoted as centroid method). The centroid for a set of documents is calculated

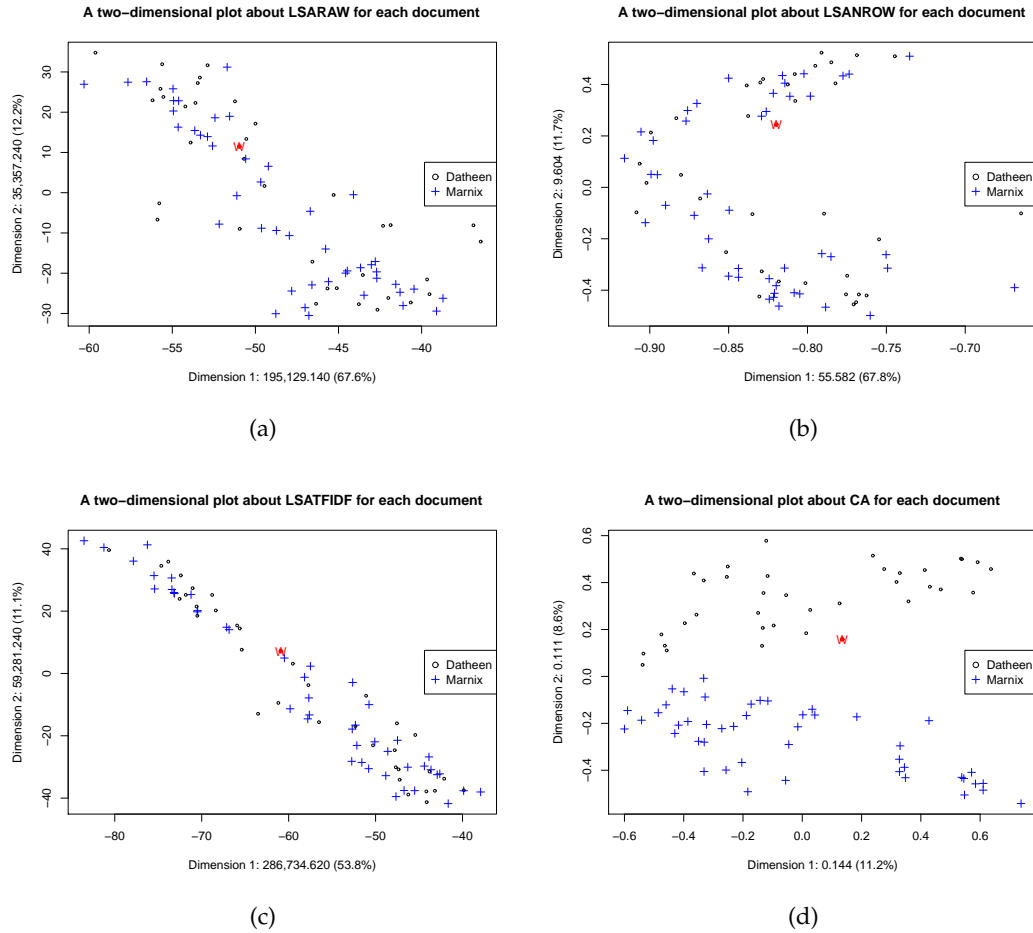


Figure 6: The first two dimensions for each document of author Datheen and author Marnix, and the *Wilhelmus* (in red) by (a) LSARAW; (b) LSANROW; (c) LSATFIDF; (d) CA.

by averaging the coordinates across all these documents. In the other three methods we first calculate the Euclidean distance between the document and every document of the set of documents. Then, in the average method the distance is the average of these Euclidean distances; in the single method the distance is the minimum Euclidean distance among these Euclidean distances; and in the complete method the distance is the maximum Euclidean distance among these Euclidean distances. These four methods are similar to the procedures of measuring the distance between clusters in hierarchical clustering analysis, using the centroid, average, single, and complete linkage method respectively (Jarman, 2020).

The choice of dimensionality and distance measurement method is a crucial issue. For choosing them, we use leave-one-out cross-validation (LOOCV) (Kuzi, Shtok, & Kurland, 2016; Wong, 2015) in combination with the concept of accuracy. We determine the number of dimensions and distance measures that provide the highest accuracy in LOOCV. The 186 documents of six authors form a document-term matrix with 186 rows and 300 columns. We perform LSARAW, LSANROW, LSATFIDF, and CA on the document-term matrix to

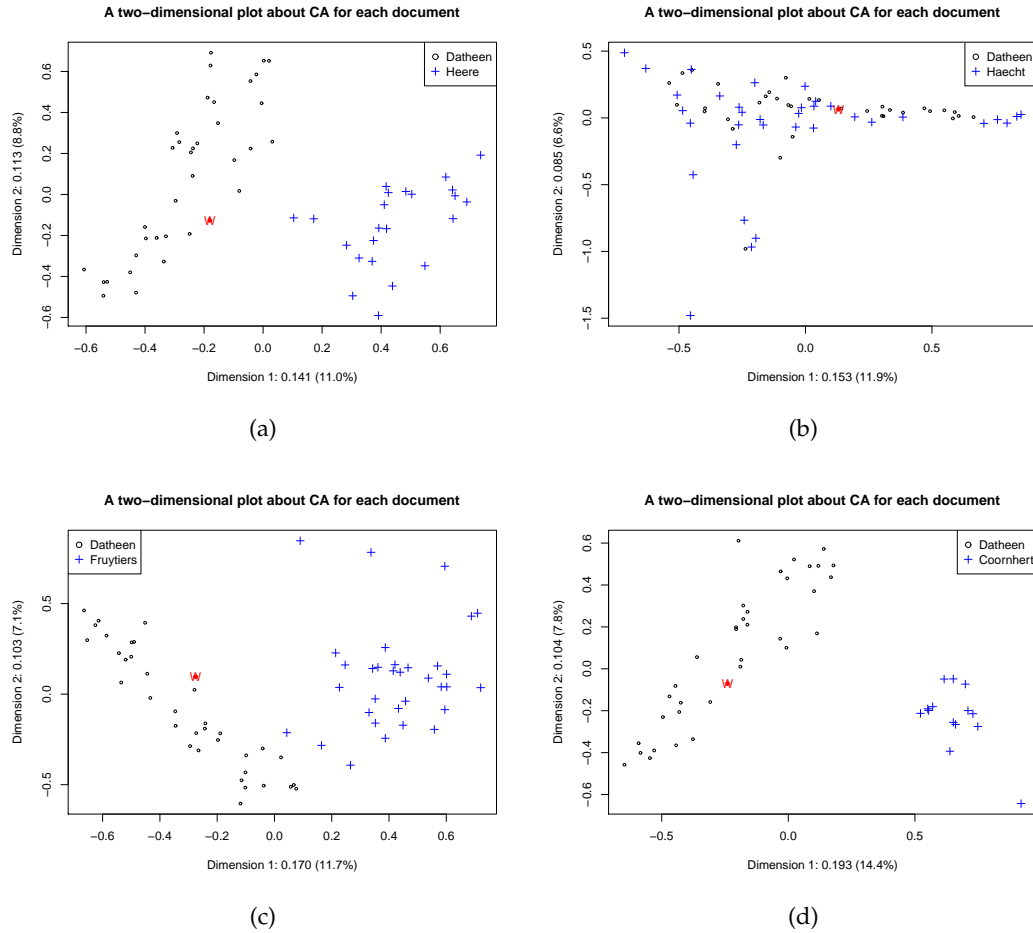


Figure 7: The first two dimensions for each document of author Datheen and another author, and the *Wilhelmus* (in red) using CA: (a) Heere; (b) Haecht; (c) Fruytiers; (d) Coornhert.

obtain the coordinates of the 186 documents in a lower dimensional space. Using LOOCV, each time we discern the following three steps. At the first step, we select one of the 186 documents. At step two, the distance is computed between the single document and all other documents from the same author using the centroid, average, single, and complete method; we predict the authorship of this single document, and the predicted author of the single document is the author with the smallest distance from the single document to all other documents of that author among all authors. At the final step, we compare the predicted author with the true author of the single document. We repeat this 186 times, once for each single documents. The accuracy is calculated by the ratio: number of times correctly predicted divided by 186.

Table 12 shows the dimensions where the maximum accuracy is reached, the size of the accuracy in the optimal dimensionality for LSARAW, LSANROW, LSATFIDE, and CA, and the accuracy for RAW, using the different distance measurement methods. From the table, the following observations can be made.

First, in the optimal dimensionality, CA yields the maximum accuracy for all dis-

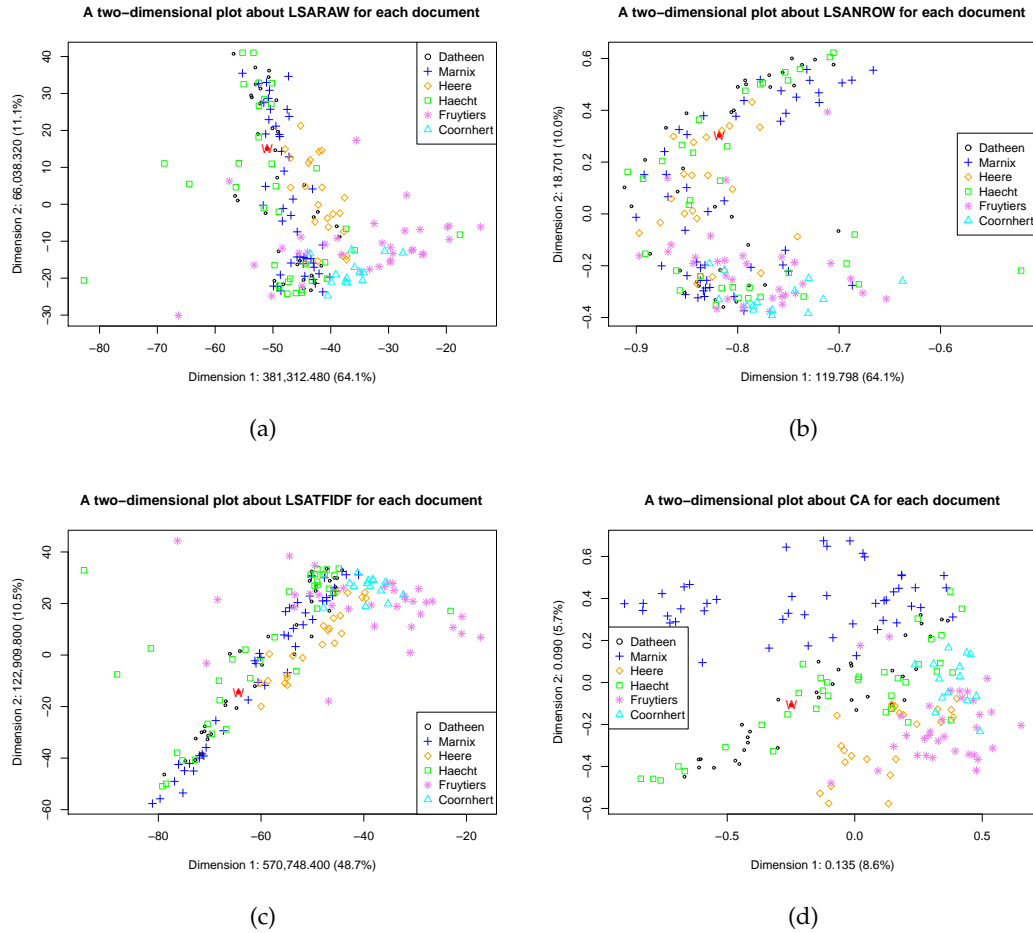


Figure 8: The first two dimensions for each document of six authors, and the *Wilhelmus* (in red) by (a) LSARAW; (b) LSANROW; (c) LSATFIDF; (d) CA.

tance measurement methods, where the accuracy for centroid method is 0.941, for average method is 0.823, for single method is 0.780, and for complete method is 0.457. This shows that we should prefer CA over the LSA methods and RAW.

Second, among all distance measurement methods, the centroid method has always the highest accuracy, for RAW with 0.720, for LSARAW with 0.720, for LSANROW with 0.747, for LSATFIDF with 0.737, and for CA with 0.941. This shows that we should prefer the centroid method over the other distance measurement methods.

In order to further explore CA, Figure 9 shows the accuracy with different numbers of dimensions using different distance measurement methods. In Figure 9(a), the dimensions are ranked from 1 to 185, and in Figure 9(b), we focus on dimensions 1 to 15. We can see that, for CA, the centroid method is best among all distance measurement methods from dimension 8 to dimension 185, where the accuracy of the centroid method is much higher than the maximum accuracy of the other methods starting at dimension 11 and the accuracy is very high over a large range.

In order to further explore the centroid method, Figure 10 shows the accuracy with different numbers of dimensions for RAW, LSARAW, LSANROW, and CA (plot of CA in

Table 12: The optimal dimensionality  $k$  and the accuracy in  $k$  for LSARAW, LSANROW, LSATFIDF, and CA, and the accuracy for RAW using different distance measurement methods.

	Centroid $k$	Centroid Accuracy	Average $k$	Average Accuracy	Single $k$	Single Accuracy	Complete $k$	Complete Accuracy
RAW		0.720		0.516		0.672		0.177
LSARAW	34–186	0.720	60;71–90	0.554	13–15	0.715	1	0.301
LSANROW	45; 46; 49–64	0.747	40	0.704	20	0.699	30; 63–186	0.296
LSATFIDF	45; 47; 52–57	0.737	19	0.543	24; 25	0.737	1	0.231
CA	56–75; 89; 90	0.941	12	0.823	14	0.780	7	0.457

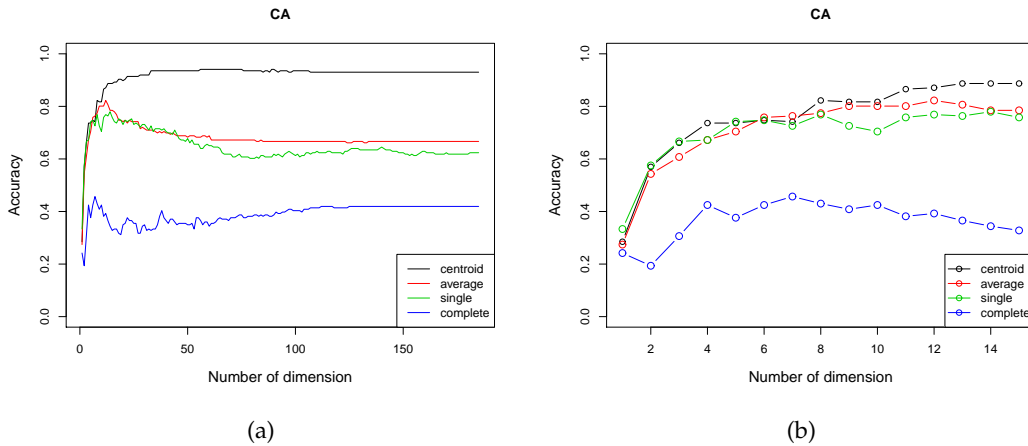


Figure 9: Accuracy versus the number of dimension for CA.

Figure 10 is the same as the plot of centroid in Figure 9.). For Figure 10(a), the dimensions are ranked from 1 to 186 (for CA 185 due to the artificial dimension that is eliminated), and for Figure 10(b), the dimensions are ranked from 1 to 10. CA in combination with the centroid method is clearly the best over all methods.

Overall, CA in combination with the centroid method appears best to study the authorship of the *Wilhelmus*. Thus we choose CA together with centroid method under its optimal dimensions (dimensions 56–75, 89, and 90) to study the authorship of the *Wilhelmus*. The Euclidean distance from the *Wilhelmus* to the centroid of all documents from Datheen is smallest among all authors and therefore, we attribute the *Wilhelmus* to Datheen.

## 7 Discussion

LSA and CA have in common that they both allow for dimensionality reduction by the SVD of a matrix. The actual matrix analysed by LSA and CA is different, and therefore LSA and CA display different kinds of information. In LSA we apply an SVD to  $F$ , or to a weighted  $F$ . In CA, an SVD is applied to the matrix  $D_r^{-\frac{1}{2}}(P - E)D_c^{-\frac{1}{2}}$  of standardized residuals. The elements in  $D_r^{-\frac{1}{2}}(P - E)D_c^{-\frac{1}{2}}$  display the departure from the margins, that is, departure from the expected frequencies under independence collected in  $E$ . Due to  $E$ , in CA the rank of  $D_r^{-\frac{1}{2}}(P - E)D_c^{-\frac{1}{2}}$  is 1 lower than the rank of  $D_r^{-\frac{1}{2}}PD_c^{-\frac{1}{2}}$ , and the

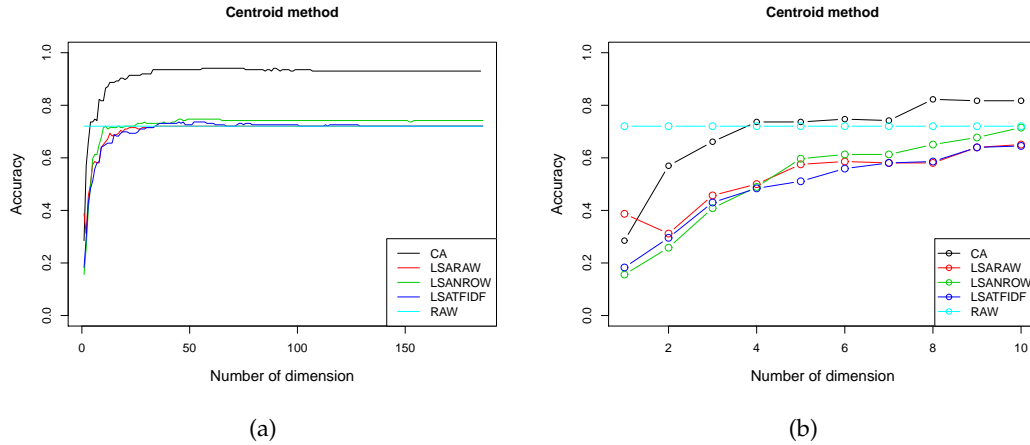


Figure 10: Accuracy versus the number of dimension for centroid method.

effect of the margins is eliminated. In CA a solution only displays the dependence between documents and terms. In LSA, the effect of the margins as well as the dependence is part of the matrix that is analysed. So, in LSA these margins usually play a dominant role in the first dimension of the LSA solution as usually on the first dimension all points depart in the same direction from the origin. On the other hand, in CA all points are scattered around the origin and the origin represents the profile of the row and column margins of  $F$ .

In summary, although LSA allows a study of the relations between documents, between terms, and between documents and terms, this study is not easy. The reason is that these relations are blurred by the effect of the margins that are also displayed in the LSA solution. CA does not have this property. Therefore it appears that CA is a better tool for studying the relations between documents, between terms, and between documents and terms. Also, discussed in Section 4, CA has many nice properties like providing a geometric display where the Euclidean distances approximate the  $\chi^2$ -distances between the rows and between the columns of the matrix, the relation to the Pearson  $\chi^2$  statistic, and the relation between CA and canonical correlation analysis that shows that CA provides the maximal correlation under all possible scorings of the row categories and column categories of the matrix. Overall, from a theoretical point of view it appears that CA has more attractive properties than LSA.

We found three mechanisms to weight documents and terms, which are weighting the matrix  $F$ , subtracting the matrix related to the row or column margins of  $F$ , and weighting documents or terms after SVD. The CA uses all three mechanisms whereas LSA usually uses only one. We have proposed a unifying framework that can include these three mechanisms and unify LSA and CA.

We also used two methods based on LSA and CA to study the authorship of the *Wilhelmus*. One is visualization by projecting documents onto two dimensions. CA does better in visualization than LSARAW, LSANROW, and LSATFIDE. In pairwise author comparisons with CA, the *Wilhelmus* is always attributed to Datheen except that in the comparison of



author Datheen and author Haecht the documents of the authors cannot be separated. The other method is to apply these methods together with distance measures. The performance of CA in combination with the centroid method outperforms that of other methods. This combination attributes the *Wilhelmus* to Datheen.

## Appendix A: Supplemental Figure

Figure A1 shows the plot of squared singular values of a document-term matrix formed by all documents from six authors. The change of behavior of squared singular values is also a sign that dimensions are enough kept. For example, from Figure A1 we can see that for LSARAW, LASNROW, and LSATFIDE, after  $k = 3$ , little squared singular values is gained, whereas for CA, after  $k = 6$ , little squared singular values is gained. In section 6.2, we do not take this as our criterion.

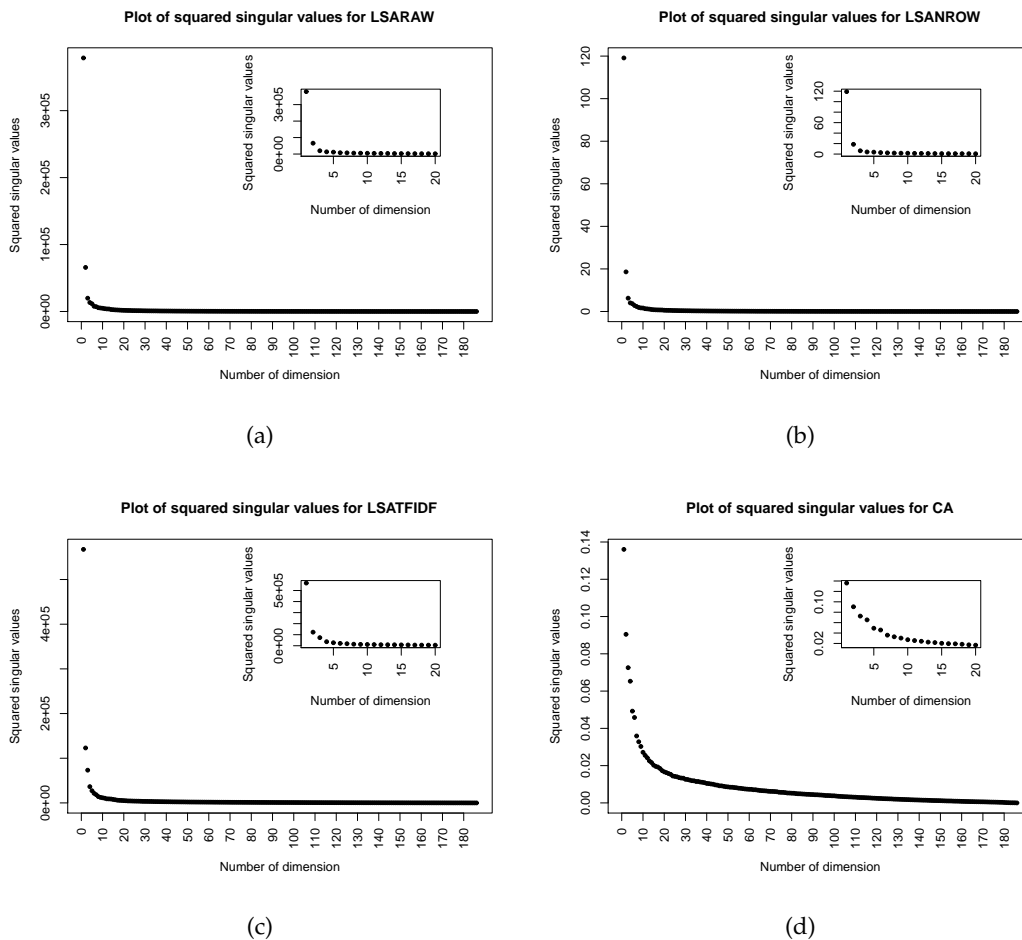


Figure A1: The plot of squared singular values from documents of six authors by (a) LSARAW; (b) LASNROW; (c) LSATFIDE; (d) CA.

## Acknowledgments

The first author is supported by the China Scholarship Council.

## References

- Ab Samat, N., Murad, M. A. A., Abdullah, M. T., & Atan, R. (2008). Term weighting schemes experiment based on SVD for Malay text retrieval. *IJCSNS*, 8(10), 357-361.
- Aggarwal, C. C. (2018). *Machine learning for text*. Springer.
- Albright, R. (2004). Taming text with the SVD. *SAS Institute Inc*.
- Benzécri, J.-P. (1973). *L'analyse des données* (Vol. 1 and 2). Dunod Paris.
- Berry, M. W., Dumais, S. T., & O'Brien, G. W. (1995). Using linear algebra for intelligent information retrieval. *SIAM review*, 37(4), 573–595.
- Bozkurt, I. N., Baghoglu, O., & Uyar, E. (2007). Authorship attribution. In *2007 22nd international symposium on computer and information sciences* (pp. 1–5).
- Deerwester, S., Dumais, S. T., Furnas, G. W., Landauer, T. K., & Harshman, R. (1990). Indexing by latent semantic analysis. *Journal of the American society for information science*, 41(6), 391–407.
- Deisenroth, M. P., Faisal, A. A., & Ong, C. S. (2020). *Mathematics for machine learning*. Cambridge University Press.
- Dumais, S. T. (1991). Improving the retrieval of information from external sources. *Behavior Research Methods, Instruments, & Computers*, 23(2), 229–236.
- Dumais, S. T., Furnas, G. W., Landauer, T. K., Deerwester, S., & Harshman, R. (1988). Using latent semantic analysis to improve access to textual information. In *Proceedings of the sigchi conference on human factors in computing systems* (pp. 281–285).
- Gifi, A. (1990). *Nonlinear multivariate analysis*. Wiley.
- Gilula, Z., & Haberman, S. J. (1986). Canonical analysis of contingency tables by maximum likelihood. *Journal of the American Statistical Association*, 81(395), 780–788.
- Goodman, L. A. (1985). The analysis of cross-classified data having ordered and/or un-ordered categories: Association models, correlation models, and asymmetry models for contingency tables with or without missing entries. *The Annals of Statistics*, 13(1), 10–69.
- Greenacre, M. J. (1984). *Theory and applications of correspondence analysis*. Academic Press.
- Greenacre, M. J. (2017). *Correspondence analysis in practice*. CRC press.
- Greenacre, M. J., & Hastie, T. (1987). The geometric interpretation of correspondence analysis. *Journal of the American statistical association*, 82(398), 437–447.
- Guthrie, D. (2008). *Unsupervised detection of anomalous text* (Ph.D. thesis). University of Sheffield.
- Hayashi, C. (1956). Theory and example of quantification (II). *Proceedings of the Institute of Statistical Mathematics*, 4, 19–30.
- Hayashi, C. (1992). Quantification method III or correspondence analysis in medical science. *Annals of Cancer Research and Therapy*, 1(1), 17–21.

- Hill, M. O. (1973). Reciprocal averaging: an eigenvector method of ordination. *The Journal of Ecology*, 61(1), 237–249.
- Hill, M. O. (1974). Correspondence analysis: a neglected multivariate method. *Applied Statistics*, 23(3), 340–354.
- Jarman, A. M. (2020). *Hierarchical cluster analysis: Comparison of single linkage, complete linkage, average linkage and centroid linkage method*. Georgia Southern University.
- Kestemont, M., Stover, J., Koppel, M., Karsdorp, F., & Daelemans, W. (2016). Authenticating the writings of Julius Caesar. *Expert Systems with Applications*, 63, 86–96.
- Kestemont, M., Stronks, E., De Bruin, M., & Winkel, T. d. (2017a). Did a poet with donkey ears write the oldest anthem in the world? Ideological implications of the computational attribution of the Dutch national anthem to Petrus Dathenus. In *DH*.
- Kestemont, M., Stronks, E., De Bruin, M., & Winkel, T. d. (2017b). *Van wie is het wilhelmus? De auteur van het nederlandse volkslied met de computer onderzocht*. Amsterdam University Press.
- Kolda, T. G., & O’leary, D. P. (1998). A semidiscrete matrix decomposition for latent semantic indexing information retrieval. *ACM Transactions on Information Systems*, 16(4), 322–346.
- Koppel, M., & Seidman, S. (2013). Automatically identifying pseudepigraphic texts. In *Proceedings of the 2013 conference on empirical methods in natural language processing* (pp. 1449–1454).
- Kuzi, S., Shtok, A., & Kurland, O. (2016). Query expansion using word embeddings. In *Proceedings of the 25th acm international on conference on information and knowledge management* (pp. 1929–1932).
- Mannion, D., & Dixon, P. (2004). Sentence-length and authorship attribution: the case of Oliver Goldsmith. *Literary and Linguistic Computing*, 19(4), 497–508.
- McCarthy, P. M., Lewis, G. A., Dufty, D. F., & McNamara, D. S. (2006). Analyzing writing styles with Coh-Metrix. In *Flairs conference* (pp. 764–769).
- Mealand, D. L. (1995). Correspondence analysis of Luke. *Literary and linguistic computing*, 10(3), 171–182.
- Mealand, D. L. (1997). Measuring genre differences in Mark with correspondence analysis. *Literary and Linguistic Computing*, 12(4), 227–245.
- Michailidis, G., & De Leeuw, J. (1998). The Gifi system of descriptive multivariate analysis. *Statistical Science*, 307–336.
- Morin, A. (1999). *Knowledge extraction in texts: a comparison of two methods*. Retrieved July 17, 2021, from <https://www.stat.fi/isi99/proceedings/arkisto/varasto/mori0673.pdf>.
- Murtagh, F., Pianosi, M., & Bull, R. (2016). Semantic mapping of discourse and activity, using Habermas’s theory of communicative action to analyze process. *Quality & Quantity*, 50(4), 1675–1694.
- Nakov, P., Popova, A., & Mateev, P. (2001). Weight functions impact on LSA performance. *EuroConference RANLP*, 187–193.

- Salton, G., & Buckley, C. (1988). Term-weighting approaches in automatic text retrieval. *Information processing & management*, 24(5), 513–523.
- Satyam, A., Dawn, A. K., & Saha, S. K. (2014). A statistical analysis approach to author identification using latent semantic analysis. *Notebook for PAN at CLEF*.
- Séguéla, J., & Saporta, G. (2011). A comparison between latent semantic analysis and correspondence analysis. In *Carrie 2011 international conference on correspondence analysis and related methods*.
- Séguéla, J., & Saporta, G. (2013). A hybrid recommender system to predict online job offer performance. *Revue des Nouvelles Technologies de l'Information, RNTI-E-25*, 177-197.
- Soboroff, I. M., Nicholas, C. K., Kukla, J. M., & Ebert, D. S. (1997). Visualizing document authorship using n-grams and latent semantic indexing. In *Proceedings of the 1997 workshop on new paradigms in information visualization and manipulation* (pp. 43–48).
- Stamatatos, E. (2009). A survey of modern authorship attribution methods. *Journal of the American Society for information Science and Technology*, 60(3), 538–556.
- Van der Heijden, P. G. M., De Falguerolles, A., & De Leeuw, J. (1989). A combined approach to contingency table analysis using correspondence analysis and loglinear analysis. *Applied Statistics*, 38(2), 249–292.
- Vargas Quiros, J. (2017). *Information-theoretic anomaly detection and authorship attribution in literature* (Master's thesis). Utrecht University.
- Winkel, T. d. (2015). *Of Deutsches blood* (Master's thesis). Utrecht University.
- Wong, T.-T. (2015). Performance evaluation of classification algorithms by k-fold and leave-one-out cross validation. *Pattern Recognition*, 48(9), 2839-2846.